20. On Earth, annually averaged meridional heat transport peaks at mid-latitudes at ~200 MW m^{-1} of which about a quarter is transported by ocean currents; see, for example, R. McIlveen, *Fundamentals of Weather and Climate* (Chapman & Hall, London, 1992). Titan's probably cratered landscape may prevent large-scale liquid motions [S. F. Dermott and C. Sagan, *Nature* **374**, 238 (1995)], confining liquids to lakes [R. D. Lorenz, *Planet. Space Sci.* **42**, 1 (1994)].
21. P. J. Gierasch and O. B. Toon, *J. Atmos. Sci.* **30**, 1502 (1973).
22. W. R. Thompson, J. A. Zollweg, D. H. Gabis, *Icarus* **97**, 187 (1992); L. C. Kouvaris and F. M. Flasar, *ibid.* **91**, 112 (1991); J. I. Lunine and D. J. Stevenson, *Nature* **317**, 238 (1985).
23. S. Engel, J. I. Lunine, W. K. Hartmann, *Planet. Space Sci.* **43**, 1059 (1995).
24. R. D. Lorenz, *ibid.* **44**, 1021 (1996).
25. J.I.L. and C.P.M. were supported through the NASA Planetary Atmospheres and Geology-Geophysics programs, and R.D.L. through the Cassini project.

3 September 1996; accepted 18 December 1996

Earth-Based Radio Tracking of the Galileo Probe for Jupiter Wind Estimation

W. M. Folkner, R. A. Preston, J. S. Border, J. Navarro*, W. E. Wilson, M. Oestreich

Although the Galileo probe was designed to communicate only to the orbiter, the probe radio signal was detected at two Earth-based radio observatories where the signal was a billion times weaker. The measured signal frequency was used to derive a vertical profile of the jovian zonal wind speed. Due to the mission geometry, the Earth-based wind estimates are less sensitive to descent trajectory errors than estimates based on probe-orbiter Doppler measurements. The two estimates of wind profiles agree qualitatively; both show high wind speeds at all depths sampled.

On 7 December 1995 the Galileo probe entered the atmosphere of Jupiter. One of the goals of the probe mission was to determine the jovian zonal (east-west) wind speed as a function of altitude by measurements of the Doppler shift of the probe radio signal received by the orbiter. Prior to the Galileo mission, various combinations of Doppler, radio interferometric, and in situ measurements of atmospheric probes from the Pioneer, Venera, and Vega missions have been used to investigate the wind speed on Venus (*1*). Remote observations of Jupiter's clouds show complex structure and large variation in wind speed (*2*). The remote observations do not penetrate the upper cloud layers and cannot determine whether the winds are driven by solar energy, which is largely absorbed in the upper cloud layers or by Jupiter's internal energy. Measurements of the Doppler shift of the probe radio signal help estimate the wind speed below the levels where sunlight is absorbed and help determine the driving mechanism.

The Galileo orbiter was nearly directly above the probe throughout the descent to maximize the signal received by the orbiter, and thus the probe-orbiter link was nearly perpendicular to the zonal wind direction. This creates some ambiguity in interpreting the probe-orbiter Doppler shift, since vertical updrafts and downdrafts or meridional winds could cause Doppler shifts potentially as large as caused by the zonal winds (*3*). After the Galileo mission was launched, it was realized that the probe radio signal could be directly detected at Earth for at least part of its descent even though the signal power was 10^9 times weaker at Earth than at the orbiter. Because the probe-Earth direction was almost parallel with the zonal wind direction, the Doppler shift as received at Earth was less sensitive to probe descent trajectory modeling than the probe-orbiter measurements (*4*).

The probe transmitted data to the orbiter on two channels near 1387 MHz (21.6 cm). Probe telemetry was sent at 256 symbols per second on each channel during the entire descent of the probe through the atmosphere with a fully suppressed carrier (*5*). One of the two probe channels was controlled by an ultra-stable oscillator (USO). This oscillator provided the frequency stability over the descent of the probe necessary to ensure that oscillator drifts were negligible compared with Doppler shifts due to changes in the wind speed. The probe carrier frequency received at the orbiter was compared to the frequency of a similar USO on the orbiter. The differenced frequency data were transmitted to Earth. Through the Doppler effect, these differenced frequency values provided a measure of relative velocity between the probe and the orbiter along the probe-orbiter direction. This velocity measurement did not represent the absolute velocity of the probe in this direction, but rather the sum of probe velocity and a (nearly) constant unknown bias, with the bias caused by the difference of the unknown frequency offsets of the probe and orbiter oscillators from their nominal frequencies.

The probe antenna pointed vertically, with the orbiter nearly overhead for best reception of the probe telemetry. Earth was near the horizon as seen from the probe. Consequently the antenna gain in the direction toward Earth was low. The power transmitted in the direction of Earth was about 60 times less than the vertical power for the first 3 min of probe transmission. As the probe descended the rotation of Jupiter caused the probe antenna to point farther from Earth so that the power transmitted toward Earth decreased to 200 times less than the vertical power 35 min after probe entry. In addition Earth was about 4000 times farther from the probe than the orbiter was.

During the probe descent, the Very Large Array (VLA) in Socorro, New Mexico, was configured to point at the Galileo probe with the signals from all 27 antennas combined to provide a collecting area equivalent to that of a 130-m diameter radio antenna. The Australia Telescope Compact Array (ATCA) in Narrabri, Australia, was similarly configured as a backup site, with its six antennas combined to form the equivalent of a 54-m diameter antenna. Since the probe signal was 100% phase-modulated by the telemetry stream, real time detection of the probe signal required sufficient signal to noise (SNR) in one symbol-time (~4 ms), which could be achieved at the orbiter but not at the Earth-based sites. Instead the Earth-based sites performed a wide band open loop recording of the probe signal for later processing. By using the known probe symbol stream, as relayed by the orbiter to Earth, the phase modulation on the probe signal due to the telemetry could be removed from the open loop recording of the probe signal, which allowed longer coherent integration times. The probe signal was successfully detected at both sites. The stronger VLA signal was used for most of the data reduction and analysis.

After removal of the telemetry modulation, the SNR at the VLA would have been adequate to determine the probe radio frequency with a simple phase-locked-loop algorithm if the signal frequency had been changing slowly enough. However the

W. M. Folkner, R. A. Preston, J. S. Border, Jet Propulsion Laboratory, California Institute of Technology, Pasadena, CA 91109, USA.
J. Navarro, National Radio Astronomy Observatory, Socorro, NM, 87801 USA.
W. E. Wilson and M. Oestreich, CSIRO Australia Telescope National Facility, Epping, New South Wales, Australia.

*Present address: Kvednaberget 12, 4033 Forus, Norway.

probe, suspended about 13 m below its parachute, was apparently swinging in a manner similar to a pendulum throughout its descent, causing continual changes in the radio frequency. This swinging of the probe was first detected in the probe transverse-accelerometer data (6), but was also seen in the probe-orbiter Doppler data (7) and in the amplitude of the probe signal received by the orbiter (8). The amplitude of the swinging caused the frequency of the probe signal as received at the VLA to change by ±5 Hz with a 5-s period (9). With this level of frequency change the VLA recording did not provide adequate SNR for carrier phase tracking. Instead, we used a signal processing technique where power spectra of the recorded signal were formed for short (0.1 s) intervals, and then averaged over 12 s (10). With this procedure the frequency variations caused by the pendulum motion were usually within a single (10 Hz) frequency bin, and averaging of independent power spectra was used to achieve adequate SNR for signal detection. This method was used to estimate the probe frequency for the first 17 min of probe transmission, during which the atmospheric pressure experienced by the probe increased from 0.4 bar to 4 bar (11). Alternate signal processing techniques show a detectable signal down to at least 7 bar.

The Earth-based detection of the probe frequency was referenced to a stable atomic clock at the radio observatories. Since the frequency of the clock was known, and the radial velocity of Jupiter relative to Earth was well known through ground-based tracking of the orbiter, the determination of the probe frequency on Earth provided a measure of the probe velocity relative to Jupiter along the probe-Earth direction. As in the case of the orbiter detection of the probe, the Earth-based velocity measurement did not provide absolute velocity of the probe in Earth direction, but rather the sum of probe velocity and a constant unknown bias arising from the unknown frequency offset of the probe's USO from its nominal frequency. Because the probe-Earth direction was nearly aligned with the zonal wind direction during the probe transmission, an offset in the probe USO frequency was not separable from a constant wind speed. The probe-orbiter geometry changed quickly enough, due to the rapid rotation of Jupiter, that differences in the probe-orbiter Doppler measurements could be used to infer the wind speed (12). This method was used to determine a zonal wind speed profile from the probe-orbiter data (7). We determined a wind profile using the probe-Earth data by including the first few seconds of the probe-orbiter Doppler measurements and assuming the nominal probe descent trajectory. The changes in the probe-orbiter Doppler measurements were used to estimate the wind speed at the beginning of the probe descent. Then, from the probe-Earth data, the probe USO frequency could be estimated along with the change in the wind speed as a function of time (13). The resulting wind profile (Fig. 1) is in qualitative agreement with the early results from the probe-orbiter measurements (7). The probe-Earth and probe-orbiter Doppler measurements show high wind speeds at depths below the regions where solar radiation is predominantly absorbed, which indicates that the winds are driven primarily by internal convection (14).

Differences in the shapes of the probe-orbiter and probe-Earth wind profiles are apparent at the beginning of the probe descent, where the probe-orbiter profile shows an initial sharp decrease in wind speed which is not seen in the probe-Earth profile, and for pressures above 2 bar, where the probe-Earth profile shows an increase of speed with depth. These differences are most likely due to differences between the nominal probe descent trajectory and the actual trajectory (15). Errors in the descent trajectory could introduce a constant bias error into the zonal wind speed estimates based on the probe-Earth data but should not affect the shape of the profile. The largest other uncertainties in the probe-Earth wind profile are due to the probe swinging motion (1 to 2 m/s), low SNR (1 to 3 m/s) and uncalibrated effects on the radio signal due to atmospheric refractivity (at Earth and Jupiter), and solar plasma (<2 m/s).

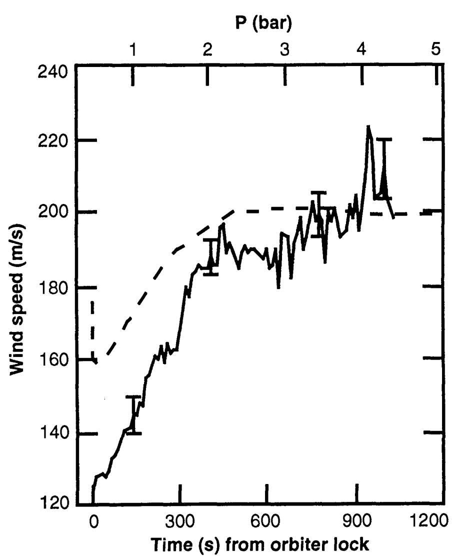

Fig. 1. Estimated Jupiter zonal wind profile from Galileo probe mission from the signal as received by the VLA (solid line). The published profile based on the probe-orbiter measurements is also shown (dotted line). Both are based on a nominal probe descent trajectory, as is the pressure scale. The error bars on the probe-Earth profile indicate measurement and modeling errors affecting changes in the wind speed. A constant bias error of about 30 m/s may exist, based on the preliminary probe descent profile; the uncertainty should be reduced to a few meters per second or less when a final descent profile is available.

The designers of the probe radio system considered the possible existence of a strongly absorbing cloud layer up to 5 km thick at about the 5-bar level. This postulated cloud layer could have caused the probe-orbiter signal power to be attenuated by as much as 2.5 times depending on the density of water and ammonia in the cloud. Had these clouds existed, the probe-Earth signal would have passed though several hundred kilometers of the cloud layer, making the probe signal undetectable. No strongly absorbing clouds were found at the probe site by in situ measurements (16) and the probe signal was detected at Earth at least down to 7 bar. At the 7-bar level the probe-Earth signal would pass through the base of the postulated cloud layer about 1400 km from the probe site, so the detection of the probe signal at Earth indicates the absence of strongly absorbing clouds far from the probe site. This is consistent with ground-based infrared observations of the probe site which show the entry site to be in a clear region of several thousand kilometers in longitudinal extent (17).

REFERENCES

1. C. C. Counselman III, S. A. Gourevitch, R. W. King, G. B. Loriot, *J. Geophys. Res.* **85**, 8026 (1980); V. V. Kerzhanovich and M. Ya. Marov, in *Venus*, M. Hunten *et al.*, Eds. (Univ. of Arizona Press, Tucson, 1983), p. 766; R. A. Preston *et al.*, *Science* **231**, 1414 (1986); R. Z. Sagdeev *et al.*, *Astron. Astrophys.* **254,** 387 (1992).
2. A. P. Ingersoll *et al.*, *J. Geophys. Res.* **86**, 8733 (1981); S. S. Limaye *et al.*, *J. Atmos. Sci.* **39**, 1413 (1982); S. S. Limaye, *Icarus* **65**, 335 (1986); R. F. Beebe, A. A. Simon, L. F Huber, *Science* **272**, 841 (1996).
3. In situ pressure and temperature measurements made by the probe, when calibrated, should determine the probe descent rate profile. Meridional winds are expected to be less than 10 m/s based on remote observations and atmospheric models but higher winds cannot be definitively ruled out without direct observations.
4. A Doppler shift of the probe frequency of 10 Hz as received by the orbiter could be due to a vertical motion of about 2 m/s, a zonal motion of about 25 m/s; or a meridional motion of about 50 m/s. A shift of 10 Hz of the probe frequency as received at Earth could be due to a vertical motion of about 6 m/s, a zonal motion of about 2 m/s, or a meridional motion of about 25 m/s. These geometric factors changed during the probe descent as the relative geometry of the probe, orbiter, and Earth changed.
5. The probe telemetry rate was 128 bits/s on each channel. The telemetry was encoded as two symbols per bit to allow for error correction.
6. A. D. Seiff *et al.*, *Science* **272**, 844 (1996).
7. D. H. Atkinson, J. B. Pollack, A. Seiff, *ibid.*, p. 842.
8. R. Woo, personal communication.

9. Because the probe antenna was not on the probe spin axis, spinning of the probe caused a similar, but smaller, effect.
10. By processing the VLA data in 0.1-s segments, the probe swinging is not resolved in the 10-Hz frequency bins. Processing the data in 1-s segments is possible and does show the probe swing in the received frequency. Longer segments were not used in the wind profile reported here due to processing time constraints.
11. The pressure of 0.4 bar occurs 20 km above the reference 1-bar level while 4 bar and 7 bar are 50 km and 75 km below the 1-bar level, respectively.
12. D. Atkinson, thesis, Washington State University (1989); J. B. Pollack, D. H. Atkinson, A. Seiff, J. Anderson, *Space Sci. Rev.* **60**, 143 (1992).
13. The design frequency of the probe USO-driven radio frequency was 1387.0 MHz. The frequency measured prior to launch was about 300 Hz higher than nominal with a drift that was not well determined. Our detected frequency was 465 ± 25 Hz higher than nominal.
14. F. H. Busse, *Astrophys. J.* **159**, 620 (1970); *Icarus* **29**, 255 (1976); P. J. Gierasch, *ibid.*, p. 445; A. P. Ingersoll and D. Pollard *ibid.* **52**, 62 (1982); K. Zhang and G. Schubert, *Science* **273**, 941 (1996).
15. Since a constant adjustment to our wind profile has been made based on the first few seconds of probe-orbiter data, the profile should agree with the profile based on the probe-orbiter data for those first few seconds given identical modeling. Part of the difference in derived wind speed at the initial time in Fig. 1 is due to characteristics of the polynomial fit applied to the probe-orbiter profile; a revision of the probe-orbiter profile (reduction in speed of about 20 m/s) due to better understanding of the orbiter Doppler receiver accounts for the remainder of the difference. Using a revised vertical descent profile, based on calibrated in situ probe temperature and temperature measurements, the Jupiter zonal wind speed profile based on only the probe-orbiter Doppler measurements has changed from (*7*) to agree better in character with Fig. 1 and indicates a lower average wind speed by about 20 m/s. D. Atkinson, private communication (1996).
16. L. A. Sromovsky *et al.*, *Science* **272**, 851 (1996); B. Ragent *et al.*, *ibid.*, p. 854.
17. G. Orton *et al.*, *ibid.*, p. 839.

18. We thank the following for their assistance in performing this experiment; D. Atkinson for helpful comments and probe-orbiter measurements; J. Ulvestad, E. M. Standish, D. Spitzmesser, and D. Jones of JPL; R. Perley, K. Sowenski, J. Wrobel, P. Dooley, M. Claussen, B. Butler, and the VLA staff; K. Wellington, M. Kesteven, R. Ferris, and the staff of the Australia Telescope; T. McElrath, F. Nicholson, and the rest of the Galileo navigation team; M. Smith, C. Sobeck, R. Sakal, P. Garriga, D. Carlock, and the rest of the Probe Project. The Very Large Array, part of the National Radio Astronomy Observatory, is operated by the Associated Universities, Inc., under cooperative agreement with the National Science Foundation. The Australia Telescope is funded by the Commonwealth of Australia for operation as a National Facility managed by CSIRO. The research described in this paper was, in part, carried out by the Jet Propulsion Laboratory, California Institute of Technology, under a contract with the National Aeronautics and Space Administration.

21 October 1996; accepted 30 December 1996

Microscopic Growth Mechanisms for Carbon Nanotubes

Jean-Christophe Charlier,* Alessandro De Vita, Xavier Blase,† Roberto Car‡

The uncatalyzed edge growth of carbon nanotubes was investigated by first-principles molecular dynamics simulations. At experimental temperatures the open end of single-walled nanotubes closed spontaneously into a graphitic dome, which may explain why these nanotubes do not grow in the absence of transition metal catalysts. On the other hand, chemical bonding between the edges of adjacent coaxial tubes ("lip-lip" interactions) trapped the end of a double-walled nanotube in a metastable energy minimum, thus preventing dome closure. These calculations show that this end geometry exhibits a high degree of chemical activity and easily accommodates incoming carbon fragments, supporting a model of growth by chemisorption from the vapor phase.

Carbon nanotubes (*1, 2*) are attracting much interest because of their potential applications in high-performing nanoscale materials (*3, 4*) and electronic devices (*5, 6*). Synthesis techniques for C nanotubes have recently achieved high production yields as well as good control of the tube geometry (*3*). Carbon nanotubes typically grow in an arc discharge at a temperature of ~3000 K. Transition metal catalysts are generally necessary to produce single-walled nanotubes (*7*) but are not required to produce multiwalled nanotubes, suggesting different growth mechanisms. However, the growth of C nanotubes cannot be directly observed, and the underlying microscopic mechanisms are still unclear (*3*).

Institut Romand de Recherche Numérique en Physique des Matériaux, Ecublens, CH-1015 Lausanne, Switzerland.

*Permanent address: Unité de Physico-Chimie et de Physique des Matériaux, Université Catholique de Louvain, Place Croix du Sud 1, B-1348 Louvain-la-Neuve, Belgium.
†Permanent address: Département de Physique des Matériaux (UA 172), Université Claude Bernard, 43 bd. du 11 Novembre 1918, F-69622 Villeurbanne Cedex, France.
‡To whom correspondence should be addressed.

The earliest models for growth of multiwalled C nanotubes (*8, 9*) were based on topological considerations and emphasized the role of pentagonal and heptagonal rings capable of bending the straight hexagonal tubular network. The most debated issue was whether the ends of these nanotubes were open or closed during growth. In favor of the closed end mechanism, it was proposed that tubes grow by addition of atoms into the reactive pentagons present at the tip of the closed structure (*10*). However, recent experimental studies lend support to an open end growth mechanism (*11, 12*), in which the atoms located at the open end of the graphitic structure provide active sites for the capture of C atoms from the plasma phase. Any capped configuration is more stable than the open end geometry, and therefore it was proposed that the latter could be stabilized by the high electric field present at the tip (*13*). However, recent first-principles calculations (*14*) have shown that this is not the case for realistic electric fields. Moreover, it is controversial whether in multiwalled nanotubes the inner or the outer tubes grow first (*9, 15*) or whether different shells of the same tube may assist each other during growth (*16, 17*). Finally, it is not clear why the growth of single-walled nanotubes, in contrast to that of the multiwalled nanotubes, generally requires the presence of metal catalysts (*7, 12*).

In this work, we studied the microscopic mechanisms underlying the uncatalyzed growth of C nanotubes by performing first-principles molecular dynamics simulations of single- and double-walled nanotubes. In this approach (*18*) the forces acting on the atoms are derived from the instantaneous electronic ground state (*19*), which is accurately described within density functional theory in the local density approximation. We performed calculations on tubular nanotube sections terminated on one side by an open end and on the other side by H atoms that complete bonding to the two-coordinate C atoms (*20*). We considered a (10,0) "zigzag" nanotube (Fig. 1A), a (5,5) "armchair" single-walled nanotube, and a (10,0)@(18,0) "zigzag" double-walled nanotube (Fig. 2A) (*21*).

During the course of the simulation, the open end of the (10,0) single-walled tube closed into a structure with no residual two-coordinate atoms (Fig. 1, A through C). This closed structure is more stable than the initial open end structure by ~18 eV (that is, ~1.8 eV per initial two-coordinate C atom). This is still 4.6 eV less stable than the "ideal" C_{60}-hemisphere cap, which contains only hexagons and isolated pentagons. However, the time scale of our simulation prevented us from studying the further evolution of the tip geometry.

A similar calculation for the (5,5) single-walled nanotube led to tip closure into a hemi-C_{60} with an energy lowering of ~15 eV. In this case the open nanotube edge consists of dimers, rather than single atoms